Use of thallium to identify monovalent cation binding sites in GroEL

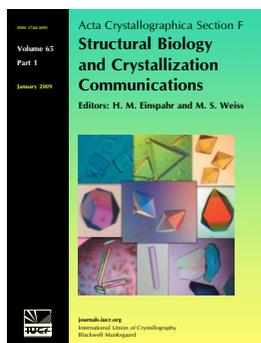Philip D. Kiser, George H. Lorimer and Krzysztof Palczewski

Crystallography Journals Online is available from **journals.iucr.org**

Use of thallium to identify monovalent cation binding sites in GroEL

Philip D. Kiser,[a] George H. Lorimer[b] and Krzysztof Palczewski[a]*

[a]Case Western Reserve University, USA, and [b]University of Maryland, USA

Correspondence e-mail: kxp65@case.edu

GroEL is a bacterial chaperone protein that assembles into a homotetradeca-meric complex exhibiting D_7 symmetry and utilizes the co-chaperone protein GroES and ATP hydrolysis to assist in the proper folding of a variety of cytosolic proteins. GroEL utilizes two metal cofactors, Mg^{2+} and K^+, to bind and hydrolyze ATP. A K^+-binding site has been proposed to be located next to the nucleotide-binding site, but the available structural data do not firmly support this conclusion. Moreover, more than one functionally significant K^+-binding site may exist within GroEL. Because K^+ has important and complex effects on GroEL activity and is involved in both positive (intra-ring) and negative (inter-ring) cooperativity for ATP hydrolysis, it is important to determine the exact location of these cation-binding site(s) within GroEL. In this study, the K^+ mimetic Tl^+ was incorporated into GroEL crystals, a moderately redundant 3.94 Å resolution X-ray diffraction data set was collected from a single crystal and the strong anomalous scattering signal from the thallium ion was used to identify monovalent cation-binding sites. The results confirmed the previously proposed placement of K^+ next to the nucleotide-binding site and also identified additional binding sites that may be important for GroEL function and co-operativity. These findings also demonstrate the general usefulness of Tl^+ for the identification of monovalent cation-binding sites in protein crystal structures, even when the quality and resolution of the diffraction data are relatively low.

1. Introduction

GroEL is an intensely studied bacterial chaperonin that together with the co-chaperonin GroES assists a variety of cytosolic proteins in reaching their native three-dimensional conformations (Houry *et al.*, 1999). In this system, a non-native substrate protein is encapsulated by a GroEL–GroES complex, where it is protected from aggregating with other non-native proteins (Horwich *et al.*, 2006). During encapsulation, it is thought that GroEL can actively unfold a non-native substrate protein, thereby giving it another chance to fold properly (Shtilerman *et al.*, 1999). After a few seconds, the system uses the power of ATP hydrolysis to expel the substrate protein, which may or may not be in its native conformation, from the cavity back into bulk solution. It is well known that GroEL exhibits both positive and negative cooperativity with respect to ATPase activity that is subject to complex allosteric regulation by several modulators (Horovitz *et al.*, 2001). Among these modulators are monovalent cations such as K^+ and NH_4^+. The effects of monovalent cations on GroEL ATPase activity are complex and depend on the presence or absence of other allosteric modulators such as substrate protein. By carefully removing other allosteric modulators, it was determined that a main effect of K^+ is to increase the affinity of GroEL for nucleotides (Grason, Gresham, Widjaja *et al.*, 2008). This increased affinity results in a shift in the midpoint of positive cooperativity to a lower ATP concentration and the appearance of negative cooperativity at higher ATP concentrations. Previous structural studies identified a metal ion coordinated by the carbonyl O atoms of Thr30 and Lys51 and a nonbridging α-phosphate O atom from the nucleotide (Boisvert *et al.*, 1996). This metal ion was suggested to be either K^+ or Ca^{2+}, but its true identity could not be ascertained owing

to similarities in the coordination chemistry and electron number of these ions and the fact that both K^+ and Ca^{2+} were present in the mother liquor from which the crystal was grown. Re-refinement of the structure using higher resolution but incomplete data resulted in metal–ligand bond distances that were more consistent with K^+ than Ca^{2+} (Wang & Boisvert, 2003). However, there is an overlap in co-ordination number and bond-length values between K^+ and Ca^{2+} and bond-length arguments based on these 2 Å resolution data cannot be considered to be definitive. In a separate crystallographic study on the asymmetric GroEL–GroES complex with bound $ADP–AlF_4$, K^+ was placed in a similar position in the structure; however, the temperature factors for these ions were around ten times higher than those of surrounding residues, making the placement of K^+ in this position questionable as well (Chaudhry *et al.*, 2003).

K^+ is the most abundant intracellular cation. Given this property, it is likely that many cytosolic proteins interact specifically with this metal cation. Indeed, the activities of several proteins, such as fructose 1,6-bisphosphatase (Hubert *et al.*, 1970), tryptophanase (Happold & Struyvenberg, 1954) and pyruvate kinase (Kachmar & Boyer, 1953) and others, in addition to GroEL (Todd *et al.*, 1993; Viitanen *et al.*, 1990) are modified by this ion. K^+ is a hard Lewis acid and consequently its interaction with protein ligands is primarily ionic in nature and often weak and transient. This presents a problem in determining the location of K^+-binding sites in protein crystal structures of moderate resolution because the ion-binding site may often be less than fully occupied, rendering the potassium ion susceptible to being confused with atoms with lower atomic number such sodium, oxygen or nitrogen. Under favorable conditions, K^+ can be differentiated from these lighter atoms by virtue of its anomalous scattering signal at longer X-ray wavelengths. However, the K^+ anomalous scattering signal is near the limits of detection at commonly used wavelengths (at 1 and 1.547 Å, $f'' = 0.47$ and $1.1 \, e^-$, respectively), making it difficult to identify in this way, especially if the diffraction data quality is less than optimal. To circumvent these difficulties, K^+ congeners or analogs, such as Rb^+, Cs^+ or Tl^+, that provide strong anomalous scattering signals are often used to replace K^+ in protein crystals. Although all of these ions have been shown to be useful for this purpose, Tl^+ has certain advantages such as an ionic radius that is more similar to that of K^+ than the others (Shannon, 1976) and a strong anomalous scattering signal at an X-ray wavelength around 1 Å, which is the region in which the flux at many synchrotron beamlines is maximal. Tl^+ has been shown to substitute structurally for K^+ in fructose-1,6-bisphosphatase (Villeret *et al.*, 1995), the K^+-ion channel (Zhou & MacKinnon, 2003) and fosfomycin-resistance protein (Rife *et al.*, 2002). Functionally, Tl^+ is able to substitute for K^+ in GroEL both in terms of its ATPase activity and in modulating its allosteric properties (Widjaja, 2002). In this study, we took advantage of previous findings that allowed us to crystallize wild-type GroEL from *Escherichia coli* in the absence of K^+ (Kiser *et al.*, 2007). We have now incorporated Tl^+ into GroEL crystals and identified its binding sites on the basis of anomalous difference Fourier electron-density maps. The data confirmed the previously suggested location of the K^+-binding site next to the nucleotide and identified two additional monovalent cation-binding sites that may be functionally relevant.

2. Experimental procedures

2.1. Purification and crystallization

Wild-type *E. coli* GroEL was purified to homogeneity as previously described (Grason, Gresham & Lorimer, 2008). Crystallization con-

Table 1
Data-collection and refinement statistics.

Values in parentheses are for the highest resolution shell.

Data collection	
Beamline	NSLS X4A
Detector	ADSC Quantum 4
Wavelength (Å)	0.97741
Temperature (K)	100
Space group	$P2_12_12_1$
Unit-cell parameters (Å)	$a = 136$, $b = 261$, $c = 288$
Resolution range (Å)	50–3.94 (4.08–3.94)
No. of unique observations	90513 (8012)
Average mosaicity (°)	0.56
Average redundancy	8.3 (5.2)
Completeness (%)	98 (88)
Average $I/\sigma(I)$	12.8 (2.1)
R_{merge}† (%)	18.9 (96)
Solvent content (%)	62
Refinement	
Refinement resolution (Å)	49.39–3.94
R_{work} (%)	26.1 [31.8]‡
R_{free}§ (%)	29.3 [34.6]‡
No. of refined atoms	
Protein	53970
ATPγS	434
Mg^{2+}	14
Tl^+	46
Overall isotropic B factor (Å^2)	125
R.m.s.d. for bond lengths (Å)	0.007
R.m.s.d. for bond angles (°)	0.919
Ramachandran plot (*PROCHECK*)	
Most favored regions (%)	90.4
Additionally allowed regions (%)	8
Generously allowed regions (%)	0.3
Disallowed region (%)	0.3

† $R_{merge} = \sum_{hkl} \sum_i |I_i(hkl) - \langle I(hkl) \rangle| / \sum_{hkl} \sum_i I_i(hkl)$. ‡ Values in square brackets are the residuals with TLS parameterization omitted. § $R_{free} = \sum_{hkl} ||F_{obs}| - |F_{calc}|| / \sum_{hkl} |F_{obs}|$ and was calculated by randomly selecting 5% of the total data.

ditions were based on those previously identified for crystallizing K^+-free native *E. coli* GroEL (Kiser *et al.*, 2007). A 70 mg ml^{-1} sample of GroEL in 10 m*M* Tris–HCl pH 7.7, 10 m*M* magnesium acetate was diluted to 15 mg ml^{-1} in deionized water for use in crystallization trials. Crystals were grown by the hanging-drop vapor-diffusion method by mixing 2 µl protein solution and 2 µl of a crystallization solution consisting of 100 m*M* Na HEPES pH 8.0, 30% 2-methyl-2,4-pentanediol (MPD) and 112 m*M* $MgCl_2$ and incubating the drop at 295 K over a well containing 1 ml of a solution identical to the crystallization solution. Crystals appeared within 1 d and grew to maximal dimensions of ∼0.8 × 0.4 × 0.05 mm within one week. To successfully carry out subsequent Tl^+ soaks it was necessary to perform the crystallization at room temperature and remove Cl^- from the crystal because Tl^+ tends to precipitate in low-temperature MPD solutions and in the presence of Cl^-. For Cl^- removal, GroEL crystals were transferred to 10 µl of a solution consisting of 100 m*M* Na HEPES pH 8.0, 30% MPD and 120 m*M* magnesium acetate and allowed to incubate for 24 h at 295 K. Crystals were then transferred to a solution consisting of 50 m*M* Na HEPES pH 8.0, 30% MPD, 50 m*M* magnesium acetate, 2 m*M* adenosine 5′-*O*-(3-thio)triphosphate (ATPγS) and 25 m*M* thallium(I) acetate and were soaked for 24 h at 295 K. Crystals were then flash-cooled in liquid nitrogen prior to X-ray exposure.

### 2.2. Data collection, structure solution and refinement

Diffraction data were collected on the National Synchrotron Light Source X4A beamline. A fluorescence scan was performed on a Tl^+-soaked GroEL crystal in order to determine the wavelength at which the anomalous scattering signal would be maximized. A data set

Table 2
Characteristics of the identified Tl⁺-binding sites.

Tl⁺-binding sites	Average σ level in final NCS-averaged anomalous difference Fourier map	Potential Tl⁺ ligands	Average distance between thallium and ligand† (Å)
Site 1: adjacent to nucleotide	11.62	α-Phosphate O atom of ATPγS	3.1 (0.17)
		γ-Phosphate O atom of ATPγS	3.0 (0.28)
		Thr30 carbonyl O atom	2.4 (0.11)
		Lys51 carbonyl O atom	3.0 (0.14)
		Thr90 O$^\gamma$ atom	3.3 (0.28)
		Thr30 O$^\gamma$ atom	3.1 (0.17)
Site 2: equatorial domain between subunits	5.59	Glu483 O$^\epsilon$ atom	2.5 (0.19)
		Asp115 O$^\delta$ atom	3.8 (0.23)
		Asn112 O$^\delta$ atom	3.2 (0.13)
		Cys458 carbonyl O atom	2.6 (0.17)
Site 3: apical domain	5.24	Phe219 phenyl C atoms	3.9 (0.26)
		Pro218 carbonyl O atom	3.6 (0.42)
		Ser217 carbonyl O atom	3.0 (0.27)
		Gln319 O$^\epsilon$ atom	3.5 (0.68)

† Values in parentheses are ± standard deviations from all observations in the asymmetric unit.

consisting of two wedges of 120 frames each was collected at a temperature of 100 K and a wavelength of 0.97741 Å, with a crystal-to-detector distance of 400 mm, an oscillation angle of 1° and an exposure time of 20 s per frame. The data were indexed, integrated and scaled, keeping the Bijvoet pairs separate, using the *HKL*-2000 software suite (Otwinowski & Minor, 1997). The crystal structure was solved by molecular replacement (MR) using the program *Phaser* (McCoy *et al.*, 2005) and a previously determined wild-type GroEL crystal structure, stripped of heteroatoms, as a search model (PDB code 1xck). The MR solution was refined with the program *REFMAC* (Murshudov *et al.*, 1997). An anomalous difference Fourier map was calculated ($|F_+| - |F_-|$, $\varphi_{model} - 90°$; Strahs & Kraut, 1968) using data to 4 Å resolution in the *CCP*4 program *FFT* in order to identify Tl⁺-binding sites (Collaborative Computational Project, Number 4, 1994).
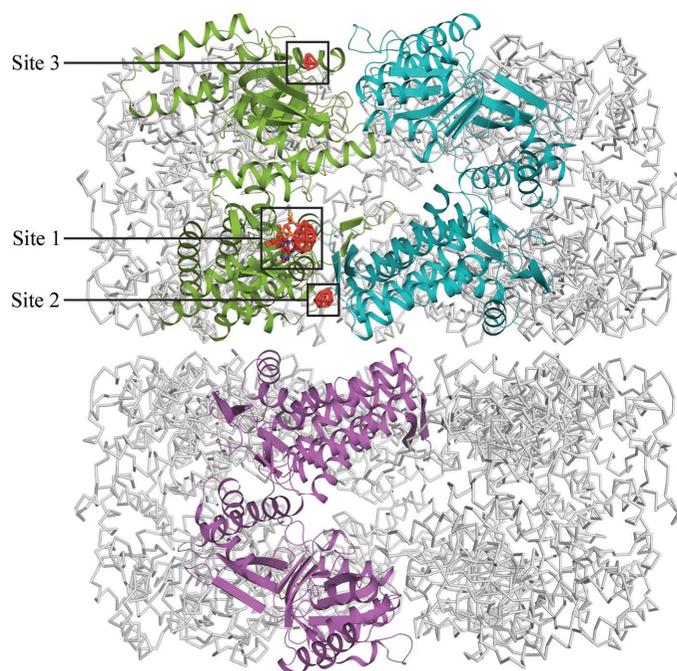
Figure 1
Overall structure of the GroEL 14-mer showing the locations of the monovalent cation-binding sites. These sites were occupied in each GroEL monomer within the complex. For clarity, only sites within one GroEL monomer are shown. The differently colored monomers show the spatial context of these monovalent cation-binding sites within the GroEL tetradecamer. Red mesh represents sevenfold NCS-averaged anomalous difference electron density contoured at 4σ.

Tl⁺ was added to the model at sites where $\geq 4\sigma$ NCS-averaged anomalous difference electron density was observed at chemically equivalent positions in a majority of the GroEL monomers. Relatively clear electron density in the nucleotide-binding region that was consistent with the presence of ATPγS was observed in every subunit of the GroEL 14-mer. An ATPγS monomer and CCP4 library were created with the *PRODRG* server (Schüttelkopf & van Aalten, 2004) and the nucleotide analog was placed in the appropriate position in every GroEL subunit. The model was further refined in *REFMAC* with 14-fold NCS restraints applied to the protein and nucleotide atoms and was manually rebuilt utilizing sevenfold NCS-averaged σ_A-weighted $2F_o - F_c$ and $F_o - F_c$ electron-density maps in the program *Coot* (Emsley & Cowtan, 2004). The overall isotropic *B* factor, which was initially set to 100 Å², was refined to a value of ~125 Å². Negative $F_o - F_c$ density was observed surrounding many of the modeled Tl⁺ sites, indicating that the occupancy at these positions was <1. Tl⁺ occupancies were manually adjusted until no negative $F_o - F_c$ density (map contoured at 3σ) was observed in each position. TLS refinement (Winn *et al.*, 2003) of the *B* factors in *REFMAC*, as described previously (Chaudhry *et al.*, 2004), was beneficial in terms of clarifying the electron-density maps and reducing R_{free}. The refinement converged to an R_{work} of 26.1% and an R_{free} of 29.3% with reasonable stereochemistry (Table 1). The model and structure-factor amplitudes have been deposited in the Protein Data Bank under accession code 3e76.

3. Results and discussion

3.1. Monovalent cation-binding sites identified in GroEL

In this study, we crystallized wild-type GroEL and introduced Tl⁺ and the poorly hydrolyzable ATP analog ATPγS into the crystal *via* soaking. Data were collected from this crystal to a resolution of 4 Å at an X-ray wavelength just above the Tl L_{III} edge in order to maximize the Tl⁺ anomalous scattering signal. The structure was solved by molecular replacement and was found to be similar to previously determined wild-type GroEL structures (Bartolucci *et al.*, 2005; Kiser *et al.*, 2007). The data quality was less than optimal as evidenced by the low resolution and relatively high R_{merge} values, but this did not affect the primary goal of this study. Four types of Tl⁺-binding sites were identified in the GroEL structure. One of these sites was found on the protein surface, mediating crystal contacts. As it is unlikely to be of functional significance, this site was not considered further.

Each of the remaining three sites was found to be occupied in every GroEL monomer of the tetradecameric complex (Fig. 1).

The strongest peaks in the anomalous difference maps were located adjacent to the nucleotide-binding site in approximately the same position as the previously suggested K^+-binding site, thus confirming this location as a genuine K^+-binding site (Fig. 2a; Chaudhry et al., 2003; Wang & Boisvert, 2003). The Tl^+ ligands are mainly the same as those identified for K^+ in the (GroEL–KMgATP)$_{14}$ structure (Wang & Boisvert, 2003; Table 2). However, there are differences in metal–ligand bond lengths between the two structures which are probably a consequence of the different chemical properties of the metal ions and nucleotides used in the respective studies. Additionally, the GroEL protein used in the previous study contained two amino-acid substitutions (R13G and A126V) which disrupt the inter-ring negative cooperativity that K^+ is known to modulate. These substitutions may have slightly altered the binding site, resulting in the observed differences in bond lengths.

The next strongest peaks in the anomalous difference map were found in the equatorial domain between GroEL monomers within a given heptameric ring. This site was formed by residues from the equatorial domains of two intra-ring GroEL monomers (Figs. 1 and 2b). The location of this site between monomers of a given ring and near the ring–ring interface is especially interesting given that K^+ and Tl^+ can influence both positive and negative cooperativity for ATP hydrolysis (Widjaja, 2002). A metal ion in this position would be uniquely situated to influence communication between and within rings of the GroEL complex. It is worth noting that in our previously determined K^+-free native GroEL structure a loop consisting of residues 474–488 that contains residues that interact with nucleotide and Tl^+ observed at this site was highly disordered, whereas in this structure the electron density for this loop is clear (Kiser et al., 2007). This may suggest that this loop is important for the communication of allosteric signals from the nucleotide-binding pocket. Further studies employing site-directed mutagenesis of residues forming this binding site will be required to determine its functional significance.

The final identified site is located in the apical domain of the protein. Ligands at this site are primarily main-chain carbonyl O atoms. There also appears to be a cation–π interaction between Tl^+ and the Phe219 side chain (Fig. 2c). Similar cation–π interactions were observed in the structure of Tl^+-derivatized fosfomycin-resistance protein (Rife et al., 2002). As the binding site is located far from the nucleotide-binding pocket and the ring–ring interface, its functional significance appears to be questionable. It is possible that this region is a nonspecific cation-binding site. However, site-directed mutagenesis studies will be required to determine the functional significance of this site.

During refinement, it was noted that the Tl^+ occupancy at all binding sites was less than one based on negative peaks in the $F_o - F_c$ electron-density maps. Although the absolute occupancy cannot be determined from the data presented here, the average σ levels for the anomalous difference maps indicate that Tl^+ in the binding site next to the nucleotide has roughly twice the occupancy of the other two sites. This observation also suggests that the binding site next to the nucleotide is likely to be the most functionally significant.

3.2. Advantages and disadvantages of Tl^+ for the identification of K^+-binding sites in proteins

The data presented here illustrate the utility of using the K^+-mimetic Tl^+ ion for X-ray crystallographic determination of K^+-binding sites in proteins even when data quality is suboptimal. As mentioned in §1, Rb^+ and Cs^+ have also been used for this purpose. Tl^+ has advantages over these K^+ congeners as well as some disadvantages that one must consider before choosing an ion for K^+ replacement in protein crystals. The principle advantages of Tl^+ over the other ions are its greater number of electrons and strong anomalous scattering signal over a wide range of X-ray wavelengths. The Tl L_{III} edge and the Se K edge are at approximately the same wavelength (∼0.979 Å), which is a region in which many synchrotron beamlines have optimized X-ray flux. Additionally, the ionic radius of Tl^+ is more similar to that of K^+ than to those of Rb^+ and Cs^+, so that Tl^+ theoretically may bind more selectively to natural K^+-binding sites than the other ions. However, use of Tl^+ also has several disadvantages that should be considered. Most importantly, Tl^+ is only slightly water-soluble in the presence of Cl^-. Addition of soluble Tl^+ salts to mother liquor containing Cl^- may reduce the Tl^+ concentration such that it is inadequate to saturate monovalent cation-binding sites in the crystal. In the present study, the best crystals required Cl^- for optimal growth, but we were able to remove excess Cl^- by soaking the crystals in Cl^--free synthetic mother liquor prior to introducing Tl^+ while still preserving the crystal integrity. Interestingly, the Tl^+ compound found in the Hampton Heavy Atom
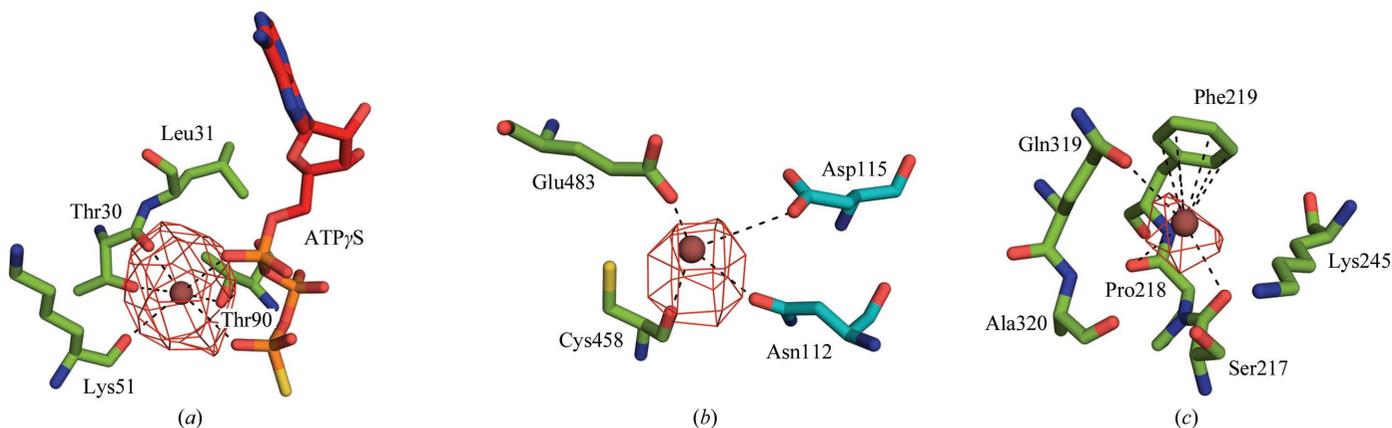
Figure 2
Potential ligands within 4.5 Å of the identified monovalent cation-binding sites. Tl^+ ions are shown as brown spheres. (a) Site 1, located next to the nucleotide, contained the strongest peaks in the anomalous difference Fourier map. (b) Site 2 is located in the equatorial domain of GroEL. This binding site, formed by a pair of intra-ring GroEL monomers (C atoms from monomers C and D are colored green and teal, respectively), is located near the ring–ring interface as shown in Fig. 1. (c) Site 3 located in the apical domain. The Tl^+ appears to form a cation–π interaction with Phe219. In each panel the NCS-averaged anomalous difference Fourier map, shown as a red mesh, is contoured at 4σ.

Screen (Hampton Research, Aliso Viejo, California, USA) is TlCl. The solubility of this compound may be too low to be useful for most applications and another salt such as acetate, nitrate, sulfate or fluoride should be used instead. Chloride salts of Rb^+ and Cs^+ are water-soluble and therefore are likely to be superior to Tl^+ if Cl^- cannot be removed from the crystal. Another disadvantage of Tl^+ is its toxicity profile compared with Rb^+ and Cs^+. Owing to its similarities to K^+, Tl^+ tends to accumulate intracellularly, where it can inhibit K^+-dependent enzymes as well as K^+ channels, leading to metabolic abnormalities and neurological injury (Galvan-Arzate & Santamaria, 1998). Accordingly, great care should be taken when handling thallium-containing compounds.

4. Summary

Use of Tl^+ in this study suggests that the highest affinity monovalent cation-binding site in GroEL crystals is located next to the nucleotide-binding site. We have also identified two additional monovalent cation-binding sites, one between monomers in the equatorial domain region and another in the apical domain. The former site may be important in modulating the allosteric properties of GroEL owing to its location between monomers near the ring–ring interface. Further mutagenesis studies will be required to test the functional significance of this site. This study demonstrates the capability of Tl^+ to substitute structurally for K^+ in a chaperonin and the utility of Tl^+ for the detection of monovalent cation-binding sites with anomalous scattering measurements even when data quality is suboptimal.

References

Bartolucci, C., Lamba, D., Grazulis, S., Manakova, E. & Heumann, H. (2005). *J. Mol. Biol.* **354**, 940–951.

Boisvert, D. C., Wang, J., Otwinowski, Z., Horwich, A. L. & Sigler, P. B. (1996). *Nature Struct. Biol.* **3**, 170–177.

Chaudhry, C., Farr, G. W., Todd, M. J., Rye, H. S., Brunger, A. T., Adams, P. D., Horwich, A. L. & Sigler, P. B. (2003). *EMBO J.* **22**, 4877–4887.

Chaudhry, C., Horwich, A. L., Brunger, A. T. & Adams, P. D. (2004). *J. Mol. Biol.* **342**, 229–245.

Collaborative Computational Project, Number 4 (1994). *Acta Cryst.* D**50**, 760–763.

Emsley, P. & Cowtan, K. (2004). *Acta Cryst.* D**60**, 2126–2132.

Galvan-Arzate, S. & Santamaria, A. (1998). *Toxicol. Lett.* **99**, 1–13.

Grason, J. P., Gresham, J. S. & Lorimer, G. H. (2008). *Proc. Natl Acad. Sci. USA*, **105**, 17339–17344.

Grason, J. P., Gresham, J. S., Widjaja, L., Wehri, S. C. & Lorimer, G. H. (2008). *Proc. Natl Acad. Sci. USA*, **105**, 17334–17338.

Happold, F. C. & Struyvenberg, A. (1954). *Biochem. J.* **58**, 379–382.

Horovitz, A., Fridmann, Y., Kafri, G. & Yifrach, O. (2001). *J. Struct. Biol.* **135**, 104–114.

Horwich, A. L., Farr, G. W. & Fenton, W. A. (2006). *Chem. Rev.* **106**, 1917–1930.

Houry, W. A., Frishman, D., Eckerskorn, C., Lottspeich, F. & Hartl, F. U. (1999). *Nature (London)*, **402**, 147–154.

Hubert, E., Villanueva, J., Gonzalez, A. M. & Marcus, F. (1970). *Arch. Biochem. Biophys.* **138**, 590–597.

Kachmar, J. F. & Boyer, P. D. (1953). *J. Biol. Chem.* **200**, 669–682.

Kiser, P. D., Lodowski, D. T. & Palczewski, K. (2007). *Acta Cryst.* F**63**, 457–461.

McCoy, A. J., Grosse-Kunstleve, R. W., Storoni, L. C. & Read, R. J. (2005). *Acta Cryst.* D**61**, 458–464.

Murshudov, G. N., Vagin, A. A. & Dodson, E. J. (1997). *Acta Cryst.* D**53**, 240–255.

Otwinowski, Z. & Minor, W. (1997). *Methods Enzymol.* **276**, 307–326.

Rife, C. L., Pharris, R. E., Newcomer, M. E. & Armstrong, R. N. (2002). *J. Am. Chem. Soc.* **124**, 11001–11003.

Schüttelkopf, A. W. & van Aalten, D. M. F. (2004). *Acta Cryst.* D**60**, 1355–1363.

Shannon, R. D. (1976). *Acta Cryst.* A**32**, 751–767.

Shtilerman, M., Lorimer, G. H. & Englander, S. W. (1999). *Science*, **284**, 822–825.

Strahs, G. & Kraut, J. (1968). *J. Mol. Biol.* **35**, 503–512.

Todd, M. J., Viitanen, P. V. & Lorimer, G. H. (1993). *Biochemistry*, **32**, 8560–8567.

Viitanen, P. V., Lubben, T. H., Reed, J., Goloubinoff, P., O'Keefe, D. P. & Lorimer, G. H. (1990). *Biochemistry*, **29**, 5665–5671.

Villeret, V., Huang, S., Fromm, H. J. & Lipscomb, W. N. (1995). *Proc. Natl Acad. Sci. USA*, **92**, 8916–8920.

Wang, J. & Boisvert, D. C. (2003). *J. Mol. Biol.* **327**, 843–855.

Widjaja, L. (2002). MS thesis. University of Maryland.

Winn, M. D., Murshudov, G. N. & Papiz, M. Z. (2003). *Methods Enzymol.* **374**, 300–321.

Zhou, Y. & MacKinnon, R. (2003). *J. Mol. Biol.* **333**, 965–975.